

# I-131 Anti-B1 Therapy/Tracer Uptake Ratio Using a New Procedure for Fusion of Tracer Images to Computed Tomography Images<sup>1</sup>

Kenneth F. Koral,<sup>2</sup> Jia Li, Yuni Dewaraja, Carla L. Barrett, Denise D. Regan, Kenneth R. Zasadny, Stephen G. Rommelfanger, Isaac R. Francis, Mark S. Kaminski, and Richard L. Wahl

Department of Internal Medicine, Division of Nuclear Medicine [K. F. K., J. L., Y. D., C. L. B., D. D. R., K. R. Z., S. G. R., R. L. W.], Department of Radiology [I. R. F.], and Department of Internal Medicine, Division of Hematology/Oncology [M. S. K.], University of Michigan Medical Center, Ann Arbor, Michigan 48109-0552

## Abstract

In patients with non-Hodgkin's lymphoma being treated by I-131-radiolabeled anti-B1 monoclonal antibody, we test the hypothesis that the activity taken up in tumors during therapy is the same as that observed during tracer evaluation, except for scaling by the ratio of administered activities. Chemotherapy-relapsed patients are imaged only with planar conjugate views, whereas previously untreated patients are imaged with planar conjugate views and with single-photon emission computed tomography (SPECT). The SPECT tracer activity quantification requires computed tomography (CT) to SPECT image fusion, for which we devised a new procedure: first, the tracer SPECT images are fused to the therapy SPECT images. Then, that transformation is combined with the therapy SPECT-to-CT transformation. We also use (a) the same volumes of interest defined on CT for both tracer and therapy image sets, and (b) a SPECT counts-to-activity conversion factor that adapts to background and rotation radius. We define  $R$  as the ratio of therapy activity percentage of infused dose over tracer activity percentage of infused dose at 2-3 days after monoclonal antibody infusion. For 31 chemotherapy-relapsed patients, the  $R$  ratio for 60 solitary or composite tumors averages  $0.931 \pm 0.031$ . The hypothesis of  $R$  being 1 is rejected with greater than 95% confidence. However, the difference from 1 is only 7.4%. The range of  $R$  is 0.43-1.55. For seven previously untreated patients,  $R$  averages  $1.050 \pm 0.050$  for

24 solitary tumors evaluated by SPECT. For six of these patients,  $R$  averages  $0.946 \pm 0.098$  for one of these solitary tumors and for five composite tumors, evaluated by conjugate views. Both results agree with the hypothesis that  $R$  is 1. The range of  $R$  for the SPECT tumors is  $0.71 \pm 0.03$  to  $1.82 \pm 0.53$ , and for the conjugate view tumors, it is  $0.70$ - $1.35$ . Plots of  $R$  versus tumor volume yield small correlation coefficients. That from SPECT approaches a statistically significant difference from zero correlation ( $P = 0.06$ ). In summary, on average, the tumor percentage of infused dose following tracer administration is predictive of therapeutic percentage of infused dose within 8%. For greater accuracy with individual tumors, however, an intratherapy evaluation is probably necessary because the range of  $R$  is large.

## Introduction

In radioimmunotherapy, it is usually assumed that an initial evaluation with a tracer amount of radiolabeled MAb<sup>3</sup> will not alter the pharmacokinetics of the biological system and will leave the tumor size unchanged. Given this assumption, the tumor uptake of activity during therapy will mimic that during the tracer evaluation, except for being larger at all time points by a given factor. The factor for the increased uptake is simply the ratio of the therapy-administered activity divided by the evaluation-administered activity. Under the assumption, the tumor radiation absorbed dose during therapy is simply the tumor dose during evaluation times this factor.

We are interested in whether tumor dosimetry can be calculated as stated above for the case of non-Hodgkin's lymphoma patients being treated by I-131-radiolabeled anti-B1 (anti-CD20) MAb. Our main focus in this paper is on previously untreated low-grade non-Hodgkin's lymphoma patients for whom individual tumor activities are assessed by SPECT imaging. We also present results from two separate conjugate view studies. One conjugate view study (1) is for salvage therapy patients of mixed grade and includes both solitary and composite tumors. The latter are groups of tumors that can be distinguished as separate by CT but are unresolved by conjugate views. The other conjugate view study is for a large subgroup of the same, previously untreated patients who are evaluated by the SPECT procedure. Again, both solitary and composite tumors are included in the conjugate view imaging.

Our SPECT imaging quantification depends upon three-dimensional "fusion," or superimposition, of the CT and the SPECT image sets (2). The edges of tumors are defined on the

<sup>1</sup> Presented at the "Seventh Conference on Radioimmunodetection and Radioimmunotherapy of Cancer," October 15-17, 1998, Princeton, NJ. Supported by United States Public Health Service Grants R01 CA38790, CA42768, and CA56794, awarded by the National Cancer Institute, National Institutes of Health, Department of Health and Human Services, and Grant M01 RR0042, awarded by the National Center for Research Resources, National Institutes of Health, Department of Health and Human Services, and by a grant from Coulter Pharmaceutical.

<sup>2</sup> To whom requests for reprints should be addressed, at University of Michigan Medical Center, R3480 Kresge III, 204 Zina Pitcher Place, Ann Arbor, MI 48109-0552. Phone: (734) 764-5103; Fax: (734) 764-0288; E-mail: kenkoral@umich.edu.

<sup>3</sup> The abbreviations used are: MAb, monoclonal antibody; SPECT, single-photon emission computed tomography; CT, X-ray computed tomography; VoI, volume of interest; RoI, region of interest; SAGE, space-alternating generalized expectation maximization; %ID, percentage of infused dose.

CT images to yield VoIs. These VoIs can be applied to the SPECT images because of the fusion. Then, "reconstructed counts" within a VoI are summed, and the total is converted to tumor activity. However, tracer reconstructed images do not carry much information, and without patient skin markers, it is difficult to fuse them to the CT image set using a mutual information algorithm. Therefore, we devised a new procedure that we describe.

## Patients and Methods

**Administered Dose.** Patients underwent the routine conjugate view imaging as part of anti-B1 trials for which they gave informed consent. The previously untreated patients who also underwent SPECT imaging gave their informed consent for the extra imaging. It was the first time the patients were being treated with anti-B1 in all cases. For the 1 week tracer evaluation, patients were given an administration of anti-B1 MAb labeled with about 5 mCi of I-131. This evaluation was then followed by the administration of a patient-specific administration of a higher-activity amount of labeled MAb. For the salvage therapy patients, a predose of 0, 95, or 475 mg of unlabeled anti-B1 MAb preceded the trace-labeled MAb. The therapy administration was preceded by the optimum amount of unlabeled predose. Similar tracer and therapy predoses were evaluated for this paper. For the previously untreated patients, the predose was always 450 mg of unlabeled anti-B1 MAb. The therapy administration was preceded by the same amount of unlabeled predose.

**Imaging.** Conjugate view imaging was usually carried out with a Siemens dual-head whole body imager. Ten min of imaging time were used for the conjugate pair of "spot" views.

SPECT imaging was accomplished with two models of a triple-headed Picker Prism rotating Anger camera. Twenty min of imaging time were used in total. Sixty projections equally spaced over 360° were acquired. A  $\pm 10\%$  photopeak, visually centered on 364 keV, was used for each head of a Prism 3000XP model when explicit scatter correction was not applied. The same window, plus a  $\pm 3\%$  low-energy window and a  $\pm 3\%$  high-energy window, was used for each head of a Prism 3000 model when triple energy window scatter correction was applied. The auxiliary windows were contiguous with the main photopeak window. Circular orbits were used for both camera models. For a given patient, the radius of rotation was usually kept at the same value for the evaluative and the intratherapy imaging.

**SPECT Reconstruction.** Because a complete set of projections covering 360 degrees was obtained for each head of the three-headed Prism Anger camera, three reconstructed image sets were obtained. Each complete projection set was separately reconstructed using the SAGE iterative algorithm (3). The same  $\beta$ -parameter value of  $2^{-10}$  was used for all patient reconstructions. This value was that used for all calibration-phantom reconstructions described in Refs. 4 and 5. The same VoI, the source of which is described below, was applied to each of the three reconstructed image sets obtained from the three heads. The section labeled SPECT data processing details how the three separate results are averaged to obtain one final estimate.

Table 1 SPECT results for *R* value for individual tumors in seven previously untreated patients

Patient no.	Tumor location	Explicit scatter correction?	Time postinfusion, $t_1$ (h)	Volume (cm <sup>3</sup> )	Activity ratio ( <i>R</i> )
13	Abdomen	No	69.6	1.6	1.27 $\pm$ 0.34
				24.6	0.95 $\pm$ 0.04
14	Abdomen	No	68.5	53.6	1.22 $\pm$ 0.07
				40.2	1.15 $\pm$ 0.07
27	Abdomen	Yes	40.3	118	0.78 $\pm$ 0.01
				153	0.90 $\pm$ 0.01
				10.5	1.00 $\pm$ 0.11
32	Abdomen	Yes	46.8	197	0.86 $\pm$ 0.04
				66.1	0.71 $\pm$ 0.03
				63.7	1.16 $\pm$ 0.06
39	Abdomen	Yes	65.5	5.9	0.85 $\pm$ 0.03
				5.1	0.78 $\pm$ 0.06
				17.0	0.86 $\pm$ 0.11
				5.0	0.74 $\pm$ 0.01
43	Abdomen	No	42.0	23.7	1.21 $\pm$ 0.21
				3.7	1.23 $\pm$ 0.24
				16.4	1.16 $\pm$ 0.06
				21.2	1.31 $\pm$ 0.17
				31.7	1.11 $\pm$ 0.03
				5.6	1.08 $\pm$ 0.14
				12.2	1.07 $\pm$ 0.13
				4.1	1.82 $\pm$ 0.53
				46.8	1.15 $\pm$ 0.12
51	Axilla	Yes	44.0	24.3	1.25 $\pm$ 0.11

**Activity Quantification.** Activity quantification with conjugate views included background regions in both views, a region size-weighted background subtraction and a patient-specific attenuation correction. The procedure for quantification of tumor activity and the required, phantom-derived curves are described in Ref. 6.

Activity quantification for the SPECT imaging is based on phantom-determined factors for conversion of reconstructed counts to activity. The factors are sensitive not only to the radius of rotation but also to a measured parameter proportional to extratumor "background" activity. Details can be found in Ref. 4 for the method without scatter correction and in Ref. 5 for the method with scatter correction. Table 1 lists seven previously untreated patients and indicates which of the two SPECT methods was used for each.

**Activity Ratio.** Ideally, the entire time activity curve for the evaluative infusion and that for the therapy infusion would be compared at multiple time points. We evaluate the ratio of therapy %ID over tracer %ID at one given time after I-131 anti-B1 infusion, usually between 2 and 3 days. That is, we evaluate the ratio *R* defined as follows:

$$R = \frac{\%ID_T}{\%ID_E}$$

Here, %ID<sub>T</sub> is the therapy %ID (*i.e.*, the tumor activity at time  $t_1$  after the therapy infusion over the therapy-infused activity decay corrected to time  $t_1$ ), and %ID<sub>E</sub> is the tracer %ID (*i.e.*, the tumor activity at the same time  $t_1$  after the evaluative infusion over the evaluative-infused activity decay corrected to time  $t_1$ ). If the actual tracer imaging time does not equal  $t_1$ , then %ID<sub>E</sub> at the actual measurement time is time interpolated to  $t_1$  so that *R*

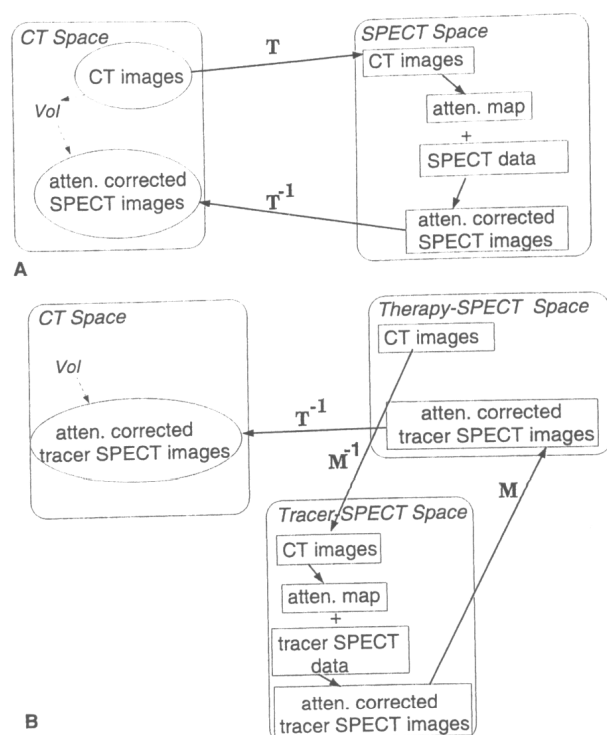


Fig. 1 Schematics for image fusion procedures. The spaces indicated are places at which all of the contained data are spatially consistent.  $T$  and  $M$  are transformations that convert image sets from one space into another. A, procedure for high-count SPECT data. These high-count data are obtained during therapy after a large administration of radioactive I-131 MAb. B, more complicated, new procedure for low-count SPECT data. These low-count data are obtained during evaluation after a tracer administration of radioactive I-131 MAb.

can be evaluated. For both SPECT and conjugate views, the shape of the tracer conjugate view time-activity curve is used to carry out the interpolation. The conjugate view data are fit using a sum of three exponentials to get the shape.

**SPECT Procedure.** The procedure that we used to quantitatively evaluate low-noise, intratherapy SPECT data is shown in Fig. 1A. The first step is to establish VoI for the tumors in the CT space. A trained radiologist (I. R. F.) identified tumors and drew the tumor RoIs on film for each transverse plane of the CT image set. A digital copy of the CT image sets was also obtained and was reduced from  $512 \times 512$  to  $256 \times 256$  for convenience. The tumor outlines were transferred to the digital data sets by redrawing with a mouse. The principal author decided which RoIs formed the VoI for a single tumor. To be combined, individual RoIs must overlap from one slice to the next or be contiguous in a single slice. (It was assumed that two adjacent cancerous lymph nodes have grown into a single tumor. Complicated, multilobulated tumors were also allowed rather than excluded. This assumption and procedural choice kept the total number of tumors down but allowed tumor shapes that are quite different from the spherical shape used in the phantom activity calibrations.)

The second step is fusion of CT images to SPECT images so that the CT images can serve as the basis for a map of

attenuation coefficients. When skin markers had not been placed at the same location in both modalities or did not show up in the images, we relied on an image brightness, mutual information (MIAMI Fuse) algorithm (7) for the required image fusion. That is the case for the patients in this report. To begin the fusion procedure, a deadtime correction was applied to each frame of the projection data. The correction assumes the paralyzable model, uses a different, measured deadtime constant for each head of the camera, and is significant only for the intratherapy data. Next, a filtered backprojection image set was reconstructed from the SPECT data. Then, a fusion of the CT images with these SPECT images was established, yielding a transformation operator,  $T$ . Using  $T$ , the CT images were brought into the SPECT space. The CT values in the transformed CT images were converted into attenuation coefficients by a formula given in Ref. 2. As the third step, the SPECT raw data were reconstructed again, this time with an attenuation correction based on the attenuation coefficient map. The SAGE iterative algorithm includes or neglects a correction for scatter depending on which Prism camera is used. As the final step, the attenuation-corrected SPECT image set was transformed back into the CT space using the transformation  $T^{-1}$ , the inverse of  $T$ . Then, the VoI defined on the digital CT images was applied to the SPECT images to obtain reconstructed counts for the tumor as a whole by summing the SPECT pixel values within the VoI.

When the SPECT data were from high-noise, first-week, intraevaluation imaging, it was difficult to accurately locate matching control points in the reference and homologous data sets, as required. However, as a whole set, the reconstructed tracer SPECT images did bear a strong resemblance to the reconstructed therapy SPECT images. Therefore, a new fusion method was used. This method is shown in Fig. 1B. Prerequisites were as follows: (a) the transformation  $T^{-1}$  from the fusion of CT images with intratherapy SPECT images as shown in Fig. 1A; and (b) the CT images after transformation to therapy SPECT space. In the first step of the new method, a tracer filtered backprojection image set was reconstructed from the tracer SPECT raw data. Then, a fusion of these SPECT images with the intratherapy SPECT images was established, yielding transformation operator  $M$ . Next, the CT images were brought from the therapy SPECT space to the tracer SPECT space using the transformation  $M^{-1}$ . They were used to generate a map of attenuation coefficients in tracer SPECT space. The tracer SPECT raw data were then reconstructed with an attenuation correction based on the map. Next, the attenuation-corrected tracer SPECT images were brought into the CT space. The technique is to first move them into therapy SPECT space using transformation  $M$  and then to further move them into the CT space using transformation  $T^{-1}$ . Once in CT space, the same VoI as for the therapy SPECT was applied to obtain tracer reconstructed counts.

The details of the tracer-to-therapy fusion itself are as follows. First, the two image sets are inspected, and an estimate is made of any shift in  $z$  to the nearest whole number of planes. The final marker set from the therapy to CT fusion for the tracer set of images is input, but with an appropriate offset in  $z$  according to the above estimate. This operation can be performed easily, as each marker can be chosen in its original

Table 2 Ratio of therapy percentage infused dose over tracer percentage infused dose (*R*)

Pretreated?	Imaging	<i>n</i>	Volume range (cm <sup>3</sup> )	Average	S.E. of <i>R</i>	Range
Yes	Conjugate view	60	8.2–759	0.931	0.031	0.43–1.55
No	SPECT	24	1.3–246	1.05	0.050	0.71 ± 0.03 to 1.82 ± 0.53
No	Conjugate view	6 <sup>a</sup>	28–349	0.946	0.098	0.70–1.35

<sup>a</sup> On average, each composite conjugate view tumor is composed of 3.67 solitary SPECT tumors.

position, the plane number can be incremented or decremented, and the new marker position can be recorded. Then, the therapy data are used as the reference set, and the tracer data are used as the homologous set in a rotate-translate optimization. It can be helpful to eliminate the first and the last slices from each image set. These slices are affected by artifactual decreases in intensity because they are near the edge of the camera. These decreases cause inconsistencies when they are to be lined up with a full-strength slice after being translated the correct amount in *z*. Usually, no scaling of one data set relative to the other is allowed because the spatial gain of the camera is assumed to be stable enough over the period of 1 week so that the true mm/pixel scale is the same for the two image sets.

If the patient has shifted up and down (in the *y* direction) within the gantry between the two SPECT imaging sessions, then additional steps need to be followed. (Such a shift is possible if, for example, the bed height above the floor level is not kept the same for the two image acquisitions.) Images in the reference image set should be cropped to the area within a square set inside the SPECT reconstruction circle. This cropping prevents the counts that are piled up at the edge of the reconstruction circle in each image set from overlaying the image circles without any *y* translation.

**SPECT Data Processing.** Three values for the activity ratio are determined, one from each of the three heads of the Prism camera. That is, the tracer and therapy %ID values from the respective reconstructions for head 1 are processed to compute an *R* ratio for head 1. Similarly, *R* estimates are obtained for heads 2 and 3. We then average the three separate values for the ratio for the three heads. We report the average as the final ratio value. A SE for the mean ratio from the average over three values is also calculated and reported. An alternative calculation would be to average %ID<sub>T</sub> over the three heads, do the same for %ID<sub>E</sub>, and then divide once to find the ratio. These two procedures do not give exactly the same results, but in cases where we tested the different answers, the results were very close to each other.

Note that the data from the three heads of the rotating SPECT camera are not handled in a completely independent way, however. All fusion transformations are derived only once using only the data from head 1. The derived transformation is then applied to the image sets from each head independently. The rationale for this procedure depends on the good spatial agreement that was observed for a point in the object volume no matter which head was used.

## Results

### Conjugate View Results for Salvage Therapy Patients.

The first row of Table 2 shows the conjugate view results for 60

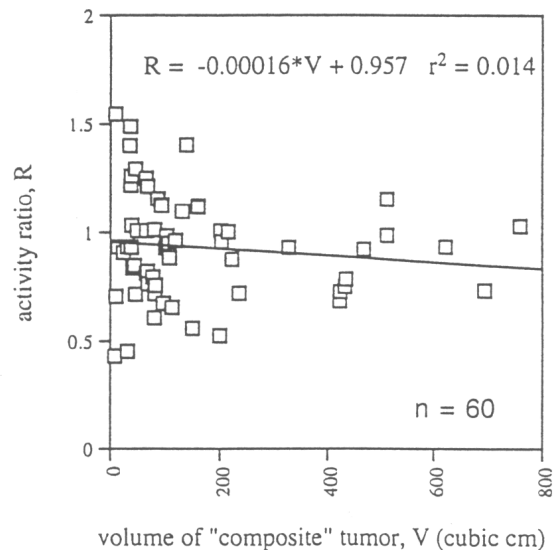


Fig. 2 Ratio of therapy %ID to tracer %ID (*R*), plotted against volume of composite or solitary tumor; shown are the conjugate view results for salvage therapy patients.

composite or solitary tumors in 31 salvage therapy patients. The average *R* value is 0.931, with a SE of only 0.031. The 95% confidence interval is 0.869–0.994. The probability of a population average of 1 is 0.03. Therefore, the hypothesis for the average ratio being 1 is rejected at the *P* = 0.03 level. However, using *R* = 1 would produce an average bias that is less than 8% [(1 – 0.931)/0.931 = 7.4%].

The range of the *R* values is 0.43–1.55. If each measured *R* value is correct, the use of the hypothetical *R* = 1 would cause an error of more than 10% in predicting therapy tumor activity from tracer tumor activity for approximately 39 of the 60 tumors (65%).

For some diseases and the applied therapy, the absorbed dose declines as the tumor volume increases (8). This effect has not been seen in anti-B1 therapy of lymphoma (9), and one would expect that even if it were seen, dependence on volume would cancel out in the *R* ratio; nevertheless, we still did investigate the correlation of the *R* value with tumor volume. This correlation is shown in Fig. 2 and yields a very small negative slope, with the square of the correlation coefficient equal to only 0.014. A Fisher's *r* to *z* transformation was carried out on the correlation coefficient to obtain a variable with a normal distribution. A *P* for the probability of the null hypothesis that the population correlation is equal to 0 was calculated.

The value is fairly large at 0.35, so there is good reason to say that no correlation with volume exists, as expected.

**SPECT Results for Previously Untreated Patients.** For the seven previously untreated patients analyzed by SPECT, the time interval between administration of the radiolabeled MAb and SPECT imaging was usually about the same for the therapy scan as for the tracer scan. The maximum time difference was 45 h for patient 13. The time-interpolation factor for this patient was 1.28. That is, her calculated tracer tumor activities were increased by this factor before the therapy-over-tracer ratio was calculated. The time-interpolation factor was less for all of the other patients.

The  $R$  values for the 24 individual tumors evaluated by SPECT are listed at the right of Table 1. The evaluation time, tumor location, and volume for each tumor are also given. The uncertainties from averaging over the three heads are largest for the smallest tumors.

The average  $R$  value is listed in Table 2. It is 1.050, with a SE of 0.050. The 95% confidence interval is 0.949–1.156. The probability of a population average of 1 is 0.30, so there is good reason to say  $R$  is 1 in this case. However, the range of  $R$  is  $0.71 \pm 0.03$  to  $1.82 \pm 0.53$ . Moreover, we see from Table 1 that if the measured  $R$  value is correct, the use of  $R = 1$  would cause an error of more than 10% in predicting therapy tumor activity from tracer tumor activity for about 19 of the 24 tumors (79%).

A plot of  $R$  value versus tumor volume for this data yields a slope of  $-0.001$ , which is more negative than that in Fig. 2. The square of the correlation coefficient is 0.093, which is larger than that in Fig. 2. The  $P$  for the probability of the null hypothesis that the population correlation is equal to 0 is only  $P = 0.064$ . It is almost but not quite small enough to say that a correlation with volume exists with 95% confidence. With more patients, SPECT might have a statistically significant correlation of  $R$  with volume. The interpretation of such a significance might more readily come from the relative accuracy of the CT-to-SPECT fusion for different size VoI than from a biological effect.

**Conjugate View Results for Previously Untreated Patients.** The  $R$  values from conjugate view analysis of tumors present in previously untreated patients are listed in Table 3. The same patients who were also imaged by SPECT are presented. (Intratherapy conjugate view data was not available for one of the seven, so that patient is missing from the table.) The tumors for the first five patients in Table 3 are composites of, on average, 4.2 individual SPECT tumors. The tumor for the last patient is a solitary tumor equivalent to the tumor evaluated by SPECT. Volumes for the composite tumors do not exactly add to the sum of the SPECT volumes because two separate digital redrawings were carried out based on the outlines on CT film. There is similarly a slight volume discrepancy for the solitary tumor. The third row of Table 2 shows that the average  $R$  value for these conjugate view tumors is 0.946 with a SE of 0.098. The 95% confidence interval is 0.694–1.198. The probability of a population average of 1 is 0.60, so there is good reason to say  $R$  is 1 in this case.

However, we see from Table 3 that if the measured  $R$  value is correct, use of  $R = 1$  would cause an error of more than 10% in predicting therapy tumor activity from tracer tumor activity for three of the six tumors (50%).

Table 3 Conjugate view results for the  $R$  value for five composite tumors and one solitary tumor in six previously untreated patients

Patient no.	Volume (cm <sup>3</sup> )	Activity ratio ( $R$ )
14	99.3	0.98
27	299	0.71
32	348	0.93
39	39.3	1.35
43	95.7	1.00
51	28.2	0.70

A plot of  $R$  versus tumor volume for this data yields a slope of  $-0.001$ , which is the same as for the SPECT data. The square of the correlation coefficient is 0.126 and thus is larger than in the SPECT case. However, the  $P$  for the probability of the null hypothesis that the population correlation is equal to 0 is also larger ( $P = 0.49$ ). Therefore, there is again good reason to say that no correlation with volume exists in this case, as was true for the previously treated patients imaged with conjugate views. This lack of correlation is as expected.

## Discussion

For patients undergoing therapy SPECT imaging, tracer-to-therapy mutual information-based fusion provides a useful method to pursue quantitative I-131 tracer SPECT without skin markers. If patients do not undergo therapy SPECT imaging, and dosimetry based on tracer SPECT and an assumed  $R$  ratio of 1 is not going to be pursued, it would be necessary to either use skin markers or to improve the information content of the tracer SPECT images. Longer imaging times plus a  $\pm 20^\circ$  orbit with a triple-head camera might accomplish the latter.

Because the activity ratio was examined at only one time point in this study, nothing can be said about the relative shape of the time activity curve after tracer infusion compared to that after the therapy infusion. However, one can say that the average  $R$  ratio is 1 within 8% at approximately day 2–3. If one assumes that the curve shapes are the same, then this study implies that inferring therapy tumor dosimetry from the tracer tumor dosimetry by multiplying by the ratio of the therapy-administered activity divided by the evaluation-administered activity will work fairly well on average. If the tracer dosimetry is available and no more is known, then this procedure appears to be reasonable.

However, with SPECT, for a given patient, the average ratio can be different from 1, and the range of the ratio for different tumors is large. If we assume that the ratios are accurate and that the results reflect a biological difference between tumors, then the inference of therapy dosimetry from tracer dosimetry using  $R = 1$  would be in error for individual tumors. Therefore, the use of an intratherapy evaluation of the uptake of each tumor at least at one time point is probably preferable to using  $R = 1$ . On the other hand, it is difficult to know whether the variability seen in  $R$  is related to the measurement technique. The precision of the registration of the tracer SPECT to the intratherapy SPECT is assumed to be “perfect” in the analysis. This assumption was not fully realized in this study, and it is indeed quite possible that minor differences in patient position between the tracer and the intratherapy SPECT

images could account for some variability. Such variability would be random but, on average, would likely result in the intratherapy scan having slightly higher I-131 tumor uptake compared to the apparent uptake on the tracer scan (the placement of the VoI on the tracer scan would likely have greater error). Indeed, the average  $R$  value is slightly greater than 1, consistent with this argument. In addition, tumor size may change in the 1-week period between the tracer image and the therapeutic image. The cause would likely be the large cold predose rather than the small radiation absorbed dose. Such a change is not accounted for in the present methods that use a single VoI for both the tracer and the therapy evaluation.

With conjugate views, the range of the ratio is also fairly large for both salvage therapy and previously untreated patients. Under the same assumptions about little error and biological difference, the use of an intratherapy evaluation of the uptake of each tumor at least at one time point is here probably somewhat preferable to using  $R = 1$ .

## Acknowledgments

We gratefully acknowledge the assistance of Chuck Meyer in providing the MIAMI Fuse program and that of Jeff Fessler in making the SAGE reconstruction program available.

## References

1. Zasadny, K. R., Gates, V. L., Moon, S., Regan, D. D., Kaminski, M. S., and Wahl, R. L. Do tracer dosimetry studies predict normal organ and tumor uptake of I-131-and-B1 (anti CD20) antibody in patients receiving radioimmunotherapy for non-Hodgkin's lymphoma? *Radiology*, 205P: 260, 1997.
2. Koral, K. F., Zasadny, K. R., Kessler, M. L., Luo, J.-q., Buchbinder, S. F., Kaminski, M. S., Francis, I., and Wahl, R. L. CT-SPECT fusion plus conjugate views for determining dosimetry in  $^{131}\text{I}$ -monoclonal antibody therapy of lymphoma patients. *J. Nucl. Med.*, 35: 1714-1720, 1994.
3. Fessler, J. A., and Hero, A. O. Penalized maximum-likelihood image reconstruction using space-alternating generalized EM algorithms. *IEEE (Inst. Elec. Electron. Eng.) Tr. Im. Proc.*, 4: 1417-429, 1995.
4. Koral, K. F., Dewaraja, Y., and Lin, S.  $^{131}\text{I}$  Tumor Quantification: A New Background-Adaptive Method. Conference Record. 1997 IEEE Medical Imaging Conference, Albuquerque, New Mexico, CD-ROM: 1155-1159.
5. Dewaraja, Y., Li, J., and Koral, K. Quantitative I-131 SPECT with triple energy window Compton scatter correction. *IEEE (Inst. Elec. Electron. Eng.) Trans. Nucl. Sci.*, 45: 3109-3114, 1998.
6. Koral, K. F., Zasadny, K. R., Swailem, F. M., Buchbinder, S. F., Francis, I. R., Kaminski, M. S., and Wahl, R. L. Importance of intratherapy single-photon emission tomographic imaging in calculating tumour dosimetry for a lymphoma patient. *Eur. J. Nucl. Med.*, 18: 432-435, 1991.
7. Meyer, C. R., Boes, J. L., Kim, B., Bland, P. H., Zasadny, K. R., Kison, P. V., Koral, K., Frey, K. A., and Wahl, R. L. Demonstration of accuracy and clinical versatility of mutual information for automatic multimodality image fusion using affine and thin-plate spline warped geometric deformations. *Med. Im. Anal.*, 1: 195-206, 1996/97.
8. Behr T. M., Sharkey R. M., Juweid M., Dunn R. M., Vagg R. C., Ying Z., Zhang C-H., Swayne L. C., Vardi Y., Seigel J. A., and Goldenberg D. M. Phase I/II clinical radioimmunotherapy with an I-131-labeled anti-carcinoembryonic antigen murine monoclonal antibody IgG. *J. Nucl. Med.*, 38: 858-870, 1997.
9. Koral K. F., Dewaraja Y., Li J., Lin S., Regan D., Zasadny K. R., Francis I., Kaminski M. S., and Wahl R. L. Preliminary report of tumor dosimetry from I-131 SPECT of previously-untreated patients with B-cell lymphoma. *J. Nucl. Med.*, 39: 112P, 1998.